Half-Site Reactivity, Negative Cooperativity, and Positive Cooperativity: Quantitative Considerations of a Plausible Model[†]

Curtis R. Bloom,[‡,§] Niels C. Kaarsholm,[∥] Julie Ha,[‡] and Michael F. Dunn*[,‡]

Department of Biochemistry, University of California, Riverside, Riverside, California 92521, and Novo Research Institute, Novo Nordisk A/S, DK-2880 Bagsvaerd, Denmark

Received April 1, 1997; Revised Manuscript Received July 16, 1997[⊗]

ABSTRACT: The nature of cooperative allosteric interactions has been the source of controversy since the ground-breaking studies of oxygen binding to hemoglobin. Until recently, quantitative examples of a model based on the inherent symmetry and asymmetry of oligomeric proteins have been lacking. This laboratory has used the phenolic ligand binding characteristics of the insulin hexamer to develop the first quantitative model for a symmetry−asymmetry-based cooperativity mechanism. The insulin hexamer possesses positive and negative heterotropic and homotropic interactions involving two classes of sites. In this study, we explore the effects of heterotropic interactions between these sites. We show that application of the pairwise structural asymmetry theory of Seydoux, Malhotra, and Bernhard (SMB) gives excellent agreement between the ligand binding behavior and X-ray crystal structure data. Furthermore, by comparing experimental data with computer simulations, we show that the insulin hexamer can be described by a three-state SMB model involving two positive homotropic cooperative transitions linked by a negative homotropic interaction. The first transition, $T_3T_3' \rightleftharpoons T_3{}^oR_3{}^o$, with allosteric constant $L_o{}^A = [T_3T_3']/[T_3{}^oR_3{}^o]$ and ligand dissociation constant $K_R{}^o$ consists of a positive cooperative change from high to low symmetry that results in "half-site reactivity". The second transition, $T_3{}^oR_3{}^o \rightleftharpoons R_3R_3'$, with allosteric constant $L_o{}^B = [T_3{}^oR_3{}^o]/[R_3R_3']$ and ligand dissociation constant K_R is a change from low to high symmetry, which is also a positive cooperative process. Treatment of the two transitions as concerted and interconnected processes allows derivation of an equation for the fraction of R-state. Using this equation, the effects of changes in the four physical parameters, $L_o{}^A$, $L_o{}^B$, K_R, and $K_R{}^o$, on the ligand binding properties of the insulin hexamer are quantitatively described.

By introducing the concept that conformational change is intimately related to protein function, Monod, Wyman, and Changeux (MWC)[1] broke new ground in describing enzyme regulatory phenomena. The classical, symmetry-conserved MWC model for ligand-linked conformational changes (Monod et al., 1965) provides a plausible explanation for several allosteric phenomena including positive homotropic interactions and the modulation of these interactions by positive and negative heterotropic effectors. However, because the subunit symmetry restrictions of the model require that bonding favor the transition to the higher affinity conformation (the T to R transition), the MWC model cannot explain negative homotropic interactions.

The treatment proposed by Koshland, Nemethy, and Filmer (KNF; Koshland et al., 1966) is often presented as an alternative to the MWC model. This treatment avoids the assumption about subunit symmetry and allows the existence of intermediate conformational forms. The KNF model further predicts that conformational change is induced in individual subunit(s) as a consequence of ligand binding and that conformational changes take place in a sequential manner. Hence, in the absence of ligands the protein exists in one conformation. Unlike the MWC model which requires only three adjustable parameters, the number of adjustable parameters allowed by the KNF system is generally equal to the number of binding sites. As a result, the KNF treatment has greater flexibility in mathematical fitting of any binding process, including negative homotropic interactions.

The term negative cooperativity is used empirically to denote binding isotherms exhibiting shapes consistent with either apparent affinities which become weaker as ligand concentration is increased or binding isotherms which appear

[†] This work was supported by a gift from the Novo Research Institute.

* To whom correspondence should be addressed.

[‡] University of California, Riverside.

[§] Current address: Department of Chemistry, California Institute of Technology, Pasadena, CA.

[∥] Novo Research Institute.

[⊗] Abstract published in *Advance ACS Abstracts,* October 1, 1997.

[1] T and R are used throughout to designate the global conformations of different allosteric conformation states. The superscripts ′ and ° denote local differences in global conformations. Z_n where $n = 0-3$ designates bound subunits in the R_o conformation state; Q_n where $n = 0-6$ designates bound subunits in the R or R′ conformations states; P designates phenolic ligands; Y_F designates the fraction of sites actually bound; $\alpha = [P]/K_R$; $\beta = [P]/K_R{}^o$. The global conformations of insulin hexamer forms with extended (T) and α-helical (R) conformations of B-chain residues 1−8 are designated as T_6, T_3R_3, and R_6 (Kaarsholm et al., 1989). T_3T_3' and R_3R_3' designate conformations with one 3-fold axis and three pseudo-2-fold axes of symmetry, while $T_3{}^oR_3{}^o$ designates the hexamer with only a single, 3-fold, axis of symmetry (Bloom et al., 1995). Abbreviations: KNF, the sequential model for allostery (Koshland et al., 1966); SMB, the half-site reactivity (suboptimal symmetry) model for cooperativity (Seydoux et al., 1974); MWC, the concerted (symmetry conserved) model for positive cooperativity (Monod et al., 1965); $L_o{}^A$ and $L_o{}^B$, allosteric constants for the interconversion of T_3T_3' with $T_3{}^oR_3{}^o$ and of $T_3{}^oR_3{}^o$ with R_3R_3', respectively; $K_R{}^o$, K_R, and K_R', dissociation constants for ligand binding to the phenolic pockets of the $R_3{}^o$, R_3, and R_3' units of $T_3{}^oR_3{}^o$ and R_3R_3', respectively; K_T, dissociation constant for the binding of phenolic ligands to trimeric units in the T-state conformation; 2,6-DHN, 2,6-dihydroxynaphthalene; PABA, *p*-aminobenzoic acid.

S0006-2960(97)00762-9 CCC: $14.00

to saturate at a site occupancy less than the total number of sites (e.g., half-site reactivity). On the basis of the observation that many oligomeric proteins and enzymes are composed of asymmetric dimers, i.e., pairs of polypeptides of identical covalent structure which have different tertiary conformation, Seydoux, Malhotra, and Bernhard (SMB; Seydoux et al., 1974) proposed a plausible structural basis for negative homotropic cooperativity. The SMB model postulates that the suboptimal symmetry can give rise to two classes of binding sites within each dimeric unit, and in the extreme, binding at one class of sites may preclude binding to the second class of sites, a condition designated as half-site reactivity (Matthews & Bernhard, 1973).

In the case of negative homotropic cooperativity in a dimeric system, it is often impossible to distinguish between a symmetry/asymmetry (SMB) and a sequential, ligand-induced (KNF) process. However, with the combination of X-ray structural information (Smith et al., 1984; Baker et al., 1988; Derewenda et al., 1989; Smith & Dodson, 1992a,b; Ciszak & Smith, 1994) and physical biochemical data (Kaarsholm et al., 1989; Roy et al., 1989; Brader et al., 1991; Choi et al., 1993; Brzovic et al., 1994), the insulin hexamer has recently emerged as an important new paradigm for the study of allostery (Bloom et al., 1995, 1997; Choi et al., 1996). The physical characteristics of the insulin hexamer allow a clear distinction between the SMB, MWC, and KNF models, and the hexamer represents the first example of a system where positive and negative cooperativity as well as half-site reactivity can be quantitatively assigned an allosteric mechanism that is based on symmetry constraints.

In the present paper we show that the applicability of the SMB model to the insulin hexamer can be extended to include heterotropic allosteric interactions. We derive quantitative expressions (see Appendix) for the SMB model tailored specifically to the insulin hexamer, and through simulation of the binding isotherms presented in the preceding paper and in work presented herein, we demonstrate how ligand binding in the insulin system is modulated both by the structure of the homotropic binding site and by the action of homotropic and heterotropic effectors.

MATERIALS AND METHODS

The insulin samples, ligands, and buffer were the same as described in the preceding paper [Bloom et al., 1997; see also Bloom et al. (1995)], as were titrations and data analysis. Simulations of ligand binding isotherms were calculated as described in the Results and Discussion section.

RESULTS AND DISCUSSION

We present our results in four parts: (1) we develop the general formalism of the SMB model in terms of conformation states, allosteric transitions, and binding equilibria specifically designed to reflect the allosteric properties of the insulin hexamer; (2) we investigate and quantify the effects of heterotropic interactions involving the synergism between ligand binding to the HisB10 metal ion sites and the phenolic pockets; (3) using the hexamer SMB model, we examine how the shapes of the titration isotherms for phenolic ligands depend on the values of the allosteric constants which describe the allosteric transitions and on the dissociation constants which describe ligand binding; and (4) we explore the effects of heterotropic interactions on the apparent values of allosteric constants and the shapes of the titration isotherms. At each stage, we compare the experimental results obtained herein and in our preceding publications (Bloom et al., 1995, 1997) with predictions derived from analysis of the model.

The Seydoux, Malhotra, and Bernhard Model. The SMB model (Seydoux et al., 1974) can be described using four basic assumptions about the structure of an oligomeric protein.

(1) Subunits or protomers comprised of identical primary sequences assemble into dimeric units about an imperfect (pseudo) 2-fold symmetry axis.

(2) The aggregation of *n* dimeric units occurs in a regular arrangement about a perfect *n*-fold symmetry axis.

(3) At least two distinct global conformations of the protomers exist for the native structure, denoted T and R in analogy to the nomenclature of MWC.

(4) The binding of ligands occurs at distinct, symmetry-related sites that are separated by large distances.

The properties of half-site reactivity, negative and positive homotropic interactions, and negative and positive heterotropic interactions occur as a consequence of these physical properties.

The Insulin Hexamer. Attempts to quantify previously reported allosteric systems exhibiting both negative and positive cooperative behavior are complicated due to ligand binding to both the T- and R-state conformations. The inability of the T-state to bind effector ligands, together with the strong allosteric interactions within the hexamer, simplifies quantitative expressions for binding.

The structural asymmetry SMB model shown in Scheme 1 (see Appendix) is capable of explaining all of the observed structural and biophysical data which characterize the insulin hexamer. Insulin hexamers are comprised of two interdigitated head-to-tail trimeric units, giving rise to three global conformation states designated T_3T_3', $T_3^oR_3^o$, and R_3R_3' (Kaarsholm et al., 1989; Bloom et al., 1995).[1] The X-ray structures of T_3T_3' and R_3R_3' hexamers derived from rhombohedral crystals[2] each possess a true 3-fold symmetry axis oriented perpendicular to three pseudo 2-fold axes (Baker et al., 1988; Smith & Dodson, 1992a). The rhombohedral $T_3^oR_3^o$ hexamer possesses a perfect 3-fold axis but no 2-fold axes of symmetry (Ciszak & Smith, 1994).[3] The HisB10 Zn^{2+} sites of the T_3, T_3^o, and T_3' units are essentially identical and usually exhibit octahedral coordination,[2] while the corresponding sites in R_3, R_3^o, and R_3' exhibit tetrahedral

[2] Due to what is presumed to be crystal lattice forces, insulin hexamer structures derived from monoclinic crystals exhibit only a pseudo-3-fold symmetry axis.

[3] The R_3 unit of the crystalline T_3R_3 complex obtained in 0.75 M Cl^- (Ciszak & Smith, 1994) appears to form a tetrahedral HisB10 site with the fourth position occupied either by Cl^- or by a water; the T_3 unit is disordered, forming either an octahedral site with three coordinated waters or a tetrahedral site with one Cl^-. The T_3 unit of the $T_3R_3-SCN^-$ complex also gives a tetrahedral zinc site; however, the fourth ligand was proposed to be a water molecule, and the density maps gave some indication of disorder at this site, consistent with some sites present in an octahedral complex. In contrast to the Zn(II)-substituted crystalline hexamer, our solution spectroscopic studies of the Co(II)-substituted hexamer support a structural assignment wherein the SCN complex gives a T_3R_3 species with SCN^- coordinated to a tetrahedral Co(II) site, presumed to be part of the R_3 unit, and an octahedral Co(II) geometry at the other HisB10 site, presumed to be part of the T_3 unit (Brader et al., 1991; Brzovic et al., 1994; Choi et al., 1996; Bloom et al., 1997).

coordination. In R_3R_3', there are two nearly identical classes of phenolic pockets, three located on R−R subunit interfaces and three located on R′−R′ subunit interfaces, whereas, in $T_3^oR_3^o$, there is a single class of three identical phenolic pockets residing on the R^o-R^o interface with a shape that is significantly different from the phenolic pockets of R_3R_3' (Bloom et al., 1997). The fourth coordination position of the HisB10 sites in the R_3, R_3^o, and R_3' units forms the loci of the anion binding sites. In each of these trimeric units, the α-helical segments of the B-chain N-termini are bundled together to form a narrow ∼12 Å deep cavity which extends from the surface along the 3-fold symmetry axis down to the Zn^{2+} site (Ciszak & Smith, 1994).

Modification of residue GluB13 to Gln by site-directed mutagenesis drastically alters the thermodynamics of the $T_3^oR_3^o$ to R_3R_3' allosteric transition of the hexamer (Roy et al., 1989; Bloom et al., 1995, 1997). Eisenstein et al. (1990) have shown that the allosteric properties of aspartate transcarbamylase can be strongly perturbed by mutation of residues at the subunit interface of this enzyme. Kuo et al. (1989) have shown that cooperativity can be introduced into *Escherichia coli* ornithine transcarbamoylase by site-directed mutagenesis, and Stebbins and Kantrowitz (1992) have reported a similar finding for the aspartate transcarbamylase from *Bacillus subtilus*.

The SMB Insulin Hexamer Model. To describe the allosteric mechanism of the insulin hexamer, we divide the conformational equilibria into two separate processes. The first consists of an equilibrium between the high-symmetry T_3T_3' state (a species with a true 3-fold axis and three pseudo 2-fold axes of symmetry) and the low-symmetry $T_3^oR_3^o$ state (with only a true 3-fold axis of symmetry) (eqs 1 and 2). The transition between these two states is defined by the allosteric constant L_o^A (Bloom et al., 1995):

$$T_3T_3' \overset{L_o^A}{\rightleftharpoons} T_3^oR_3^o \tag{1}$$

$$L_o^A = [T_3T_3']/[T_3^oR_3^o] \tag{2}$$

This transition involves a relatively stable ($L_o^A > 1$), high-symmetry state (T_3T_3') with negligible affinity for effectors (phenolic compounds and monovalent anions) and a low-symmetry state which has one class of symmetry-related, high-affinity sites (R^o) and a second class of symmetry-related very low affinity sites (T^o). As a result of side chain packing into the cryptic phenolic site, binding of phenolic ligands to the T-state is effectively rendered impossible (i.e., the ligand dissociation constant K_T approaches infinity).[1] The octahedral His(B10) Zn^{2+} site has very low affinity for anions. Provided the transition to R_3R_3' is essentially inaccessible, the binding of ligands stabilizes the low-symmetry conformation ($T_3^oR_3^o$), and saturation occurs at 50% of the total possible sites. Consequently, under appropriate conditions the insulin hexamer presents an example of a system which exhibits half-site reactivity and both negative and positive cooperativity.

The second conformational transition consists of the interconversion of the low-symmetry $T_3^oR_3^o$ state with the high-symmetry R_3R_3' state (a species with a true 3-fold axis and three pseudo-2-fold axes of symmetry). This transition (eqs 3 and 4) is defined by the allosteric constant L_o^B (Bloom et al., 1995):

$$T_3^oR_3^o \overset{L_o^B}{\rightleftharpoons} R_3R_3' \tag{3}$$

$$L_o^B = [T_3^oR_3^o]/[R_3R_3'] \tag{4}$$

Since the R_3R_3' binding sites are nearly identical, the binding of phenolic ligands occurs with essentially equivalent microscopic dissociation constants ($K_R \cong K_R'$), while the differences between the R^o and R or R′ states require a unique dissociation constant for the phenolic sites of $T_3^oR_3^o$ ($K_R^o \neq K_R' \cong K_R$). This transition is an example of a true SMB model for positive cooperativity where a state of low symmetry, with both low-affinity and high-affinity sites, is converted to a state of high symmetry, with all sites in a high-affinity state.

The combination of the two transitions defined by eqs 2 and 4 into a single, three-state system of conformational equilibria renders the insulin hexamer a unique allosteric example (eq 5) (Bloom et al., 1995; Brzovic et al., 1994). This system is comprised of mixed positive and negative cooperativity and half-site reactivity for the transition from T_3T_3' to $T_3^oR_3^o$ and of a positively cooperative transition $T_3^oR_3^o$ to R_3R_3' (eqs 5 and 6).

$$T_3T_3' \overset{L_o^A}{\rightleftharpoons} T_3^oR_3^o \overset{L_o^B}{\rightleftharpoons} R_3R_3' \tag{5}$$

$$L_o^A = [T_3T_3']/[T_3^oR_3^o] \qquad L_o^B = [T_3^oR_3^o]/[R_3R_3'] \tag{6}$$

As derived in the Appendix, the expression for the fraction of R-state for this model is given by the equation:

$$\rho = \frac{0.5L_o^B(1+\beta)^3 + (1+\alpha)^6}{L_o^B(1+\beta)^3 + (1+\alpha)^6 + L_o^AL_o^B} \tag{7}$$

[P] = concentration of the phenolic ligand, $\alpha = [P]/K_R$, and $\beta = [P]/K_R^o$.

Effects of Heterotropic Interactions between Anion and Phenolic Ligand Binding Sites on the Insulin Hexamer. Both the wild-type and the E-B13Q mutant Co(II)-substituted insulin hexamers give titration isotherms that are strongly dependent upon the structure of the phenolic ligand, the nature and concentration of the anionic ligand, and the mutation (Brader et al., 1991; Choi et al., 1993; Bloom et al., 1995, 1997). This interdependence is illustrated by the data for the E-B13Q mutant system presented in Figure 1. Owing to the mutation of GluB13 to Gln and the consequent influence of this mutation on the apparent values of L_o^A and L_o^B (Bloom et al., 1995), the initial phase of each isotherm appears nearly hyperbolic. In the presence of 25 mM Cl^-, the phenol isotherm originates at a ρ value (eq 7) of ∼0 and extrapolates to $\rho = 1.0$ at high phenol concentration (Figure 1A, □). When the anion is 5 mM PABA, the phenol isotherm originates at ρ ∼0.34 and extrapolates to $\rho = 1.0$ (Figure 1A, ■). When the phenolic ligand is 2,6-DHN (or 2,7-DHN, data not shown) and the anion is 25 mM Cl^- (Figure 1B, ◇), the isotherm exhibits an initial phase originating at a ρ value of ∼0, which tends to plateau at ρ ∼0.5, but then is followed by a second phase which increases beyond $\rho = 0.5$ at higher 2,6-DHN concentration. When carried out in the presence of 5 mM PABA (Figure 1B, ◆), the initial value of ρ again is approximately 0.34. The shape of the titration curve appears biphasic with the first phase tending to saturate at about $\rho = 0.5$, while the second phase

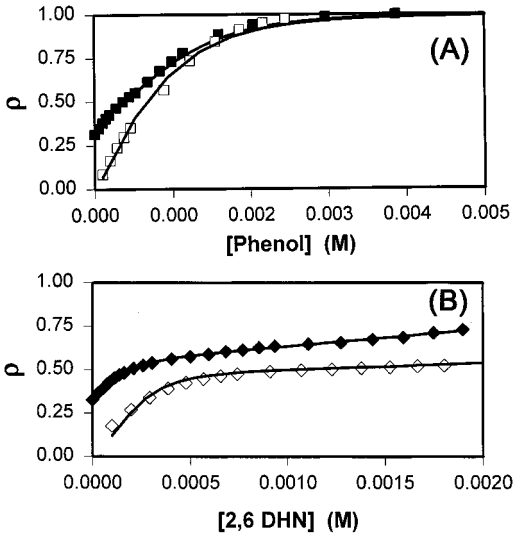

FIGURE 1: Influence of heterotropic effects on the binding isotherms for phenol (A) and 2,6-DHN (B) to E-B13Q insulin. In each panel, the solid line fitted to the open symbol (□ or ◇) is the best fit to eq 7 for the titration isotherm obtained when the ligand for the HisB10 anion binding site is Cl^- (25 mM), and the solid line fitted to the solid symbol (■ or ◆) is the best fit to eq 7 for the isotherm obtained with PABA (5 mM). The parameters, L_o^A, L_o^B, K_R, and K_R^o for each curve are given in Table 1.

Table 1: Heterotropic Effects of HisB10 Ligands on the Titration Isotherms for the Binding of Phenolic Ligands to the Co(II)-Substituted E-B13Q Mutant Insulin Hexamer[a]

HisB10 ligand	phenolic ligand	L_o^A [b]	L_o^B [b]	K_R^o [c] (M) × 10^4	K_R [c] (M) × 10^4
5 mM PABA	phenol	1.8	1.3	1.8	2.5
25 mM Cl^-	phenol[d]	25	500	1.8	1.7
5 mM PABA	2,6-DHN	2.5	1.3	2.8	8.8
25 mM Cl^-	2,6-DHN[d]	20	500	1.0	2.6

[a] A summary of allosteric constants and dissociation constants obtained from the fitting of the data is presented in Figure 1 to the SMB model (eq 7). [b] Errors in the estimated values for L_o^A and L_o^B are ±50%. [c] Errors in the estimated values for K_R^o and K_R are ±40−50%. [d] Values taken from Bloom et al. (1995).

increases to ρ values approaching 1.0 as the concentration of 2,6-DHN approaches the solubility limit, ~8 mM (data not shown).

The strong dependence of the shape of the isotherm and the initial ρ value on the anion is evidence of strong heterotropic interactions between the HisB10 anion binding sites and the phenolic pockets. As previously reported (Brader et al., 1991; Choi et al., 1993, 1996; Brzovic et al., 1994; Bloom et al., 1995), anion binding to the HisB10 sites, *in the absence of phenolic ligands*, can shift the distribution of hexamer conformations in favor of R-state species. Whittingham et al. (1995) have established that SCN^- binding to the Zn(II)-substituted hexamer gives a T_3R_3 species with a single SCN^- bound to the HisB10 site of the R_3 unit.[2] Thus, in the titration isotherms shown in Figure 1, the initial ρ values provide measures of the anion effect on the preexisting equilibrium distribution of T- and R-state species prior to addition of the phenolic ligand. As predicted by the SMB model presented in the preceding paper (Bloom et al., 1997) and more fully developed here and in the Appendix, a shift in the initial distribution in favor of R-state species gives isotherms that are increasingly hyperbolic in shape.

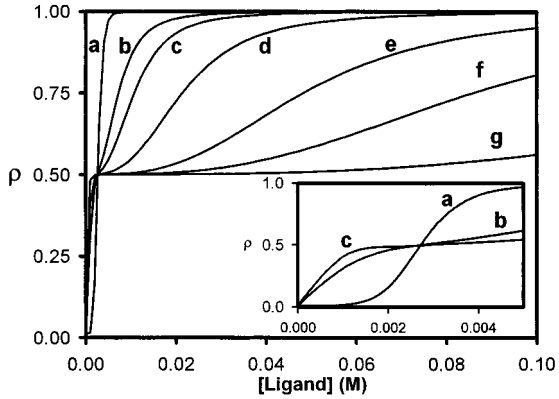

FIGURE 2: Theoretical binding isotherms for the Co(II)-substituted insulin hexamer fitted using the fraction of R-state equation (ρ) (eq 7). Isotherms are derived for values of the allosteric parameters, $L_o^A = 50$ and $L_o^B = 1 \times 10^7$, with the following values for K_R^o/K_R: (a) 1.0×10^{-3} M/1.0×10^{-4} M; (b) 3.0×10^{-4} M/1.0×10^{-4} M; (c) 2.0×10^{-4} M/1.0×10^{-4} M; (d) 1.0×10^{-4} M/1.0×10^{-4} M; (e) 1.0×10^{-4} M/1.5×10^{-4} M; (f) 1.0×10^{-4} M/(1−2.0) $\times 10^{-4}$ M; (g) 1.0×10^{-4} M/3.0×10^{-4} M.

Theoretical Modeling of Ligand Interactions. (A) Negative Homotropic Interactions. First consider how homotropic cooperativity can be manifest in the binding isotherms. Changes in the ligand structure will result in different physical and chemical interactions with the residues forming the binding sites and thus may be different for the R_3^o, R_3, and R_3' units. As a starting point for modeling, we set four parameters: $K_R^o = 1 \times 10^{-4}$ M, $K_R = K_R' = 1 \times 10^{-4}$ M, $L_o^A = 50$, and $L_o^B = 1 \times 10^7$, values comparable to those found from fitting the phenol−wild-type insulin hexamer isotherms (Bloom et al., 1995, 1997); the resulting theoretical isotherm (Figure 2, trace d) is distinctly biphasic, demonstrating negatively homotropic behavior. The SMB model predicts that negative homotropic interactions arise from ligand binding to a dimeric unit with an inherent asymmetry that results in two classes of binding sites (i.e., $K_R^o \neq K_R \cong K_R'$). In the extreme, half-site reactivity results when binding to the lower affinity sites is negligible (when $K_R^o < K_R \cong K_R'$). Figure 2 (traces d through g) shows theoretical isotherms calculated for the case where the values for K_R^o, L_o^A, and L_o^B are fixed and the dissociation constant for the R_3R_3' binding sites (K_R) is progressively raised from 1×10^{-4} to 3×10^{-4} M (a condition analogous to the 2,6-DHN−wild-type insulin hexamer). The biphasic isotherm (trace d) converts to an apparent single phase curve (trace g), saturating at half-site reactivity. Lowering the affinity for the R_3R_3' state causes the $T_3^oR_3^o$ conformation to become increasingly more stable until it is the only significant species contributing to the isotherm (Figure 2, trace g).

(B) Positive Homotropic Interactions. According to both the MWC and SMB models, positive homotropic interactions arise from the stabilization of high-symmetry, high-affinity oligomeric structures. Increasing the dissociation constant, $K_R^o > K_R' \cong K_R$, results in an apparent positive cooperative isotherm. With the initial values of $K_R^o = 1 \times 10^{-4}$ M, $K_R = K_R' = 1 \times 10^{-4}$ M, $L_o^A = 50$, and $L_o^B = 1 \times 10^7$ and the progressive raising of the dissociation constant for the $T_3^oR_3^o$ binding sites (K_R^o) to 1×10^{-3} M, the isotherms (Figure 3, traces e to a) are transformed from a biphasic curve to a full-site, monophasic, highly sigmoidal curve. The increase in K_R^o effectively destabilizes the $T_3^oR_3^o$−ligand complexes relative to the R_3R_3'−ligand complexes; therefore, $T_3^oR_3^o$

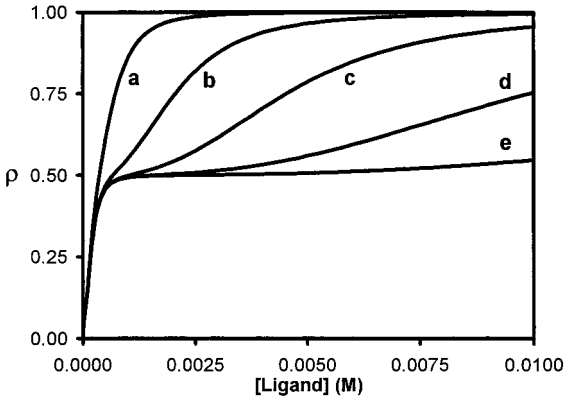

FIGURE 3: Theoretical binding isotherms for the Co(II)-substituted insulin hexamer fitted using the fraction of R-state equation (ρ) (eq 7). Isotherms are derived for $L_o^A = 50$, $K_R^o = 1 \times 10^{-4}$ M, and $K_R = 1 \times 10^{-4}$ M and the following values for L_o^B: (a) 500; (b) 1.0×10^4; (c) 1.0×10^5; (d) 1.0×10^6; (e) 1.0×10^7.

species do not significantly contribute to the isotherm. In the limiting cases (where $K_T = \infty$ or where $K_T >> K_R^o > K_R$), the SMB model for a positively homotropic cooperative hexamer becomes equivalent to the MWC model.

(C) The Preexisting Equilibrium. For the insulin hexamer system, the degree of apparent negative, positive, or half-site cooperativity observed is sensitive both to the preexisting conformational equilibria and to the relative affinities of the R^o, R, and R′ states for ligands (viz., Figure 1). This sensitivity is quantified by the magnitudes of the allosteric constants, L_o^A and L_o^B, and the dissociation constants, K_R^o, K_R, and K_R'. The values of L_o^A and L_o^B are controlled by the relative free energies of each conformation and have been shown to be drastically altered by mutation ($\Delta L_o^B > 1 \times 10^7$; Bloom et al., 1995, 1997) or by anion binding to the His(B10) sites (Figure 1). It can be shown that eq 9 can be extended to predict the initial ρ value (ρ_o) measured in the absence of phenolic ligands. Hence, ρ_o values predicted by the allosteric model developed in Scheme 1 are given by the equation:

$$[\text{R-state}]/[\text{T-state}] = \rho_o = \frac{0.5(1/L_o^A) + (1/L_o^A L_o^B)}{0.5(1/L_o^A) + 1} \quad (8)$$

To explore the dependence of curve shape on the position of the preexisting equilibrium among states by simulation, we begin by setting the R-state affinities equal to each other ($K_R = K_R^o = K_R' = 1 \times 10^{-4}$ M) for the fraction of R-state equation (ρ) and by setting $L_o^A = [T_3T_3']/[[T_3^oR_3^o] = 20$ and $L_o^B = [T_3^oR_3^o]/[R_3R_3'] = 500$ (values comparable to those obtained for the E-B13Q mutant in the presence of 25 mM Cl^-) (Figure 3a). Under these conditions, positive cooperative, full-site reactivity behavior is observed as a single, slightly sigmoidal isotherm that approaches conversion of 100% of the hexamer to the R_3R_3' state. By maintaining the above values of L_o^A, K_R, K_R^o, and K_R' while increasing the value of L_o^B from 500 to 1×10^7 (a value analogous to that of the phenol−wild-type insulin hexamer), we found that the isotherms become increasingly biphasic in character and approach an apparent half-site reactivity limit (Figure 3b−e). When $L_o^A = 20$ and $L_o^B = 1 \times 10^7$, the transition from the T_3T_3' state to the $T_3^oR_3^o$ state is easily achieved by the mass action of ligand binding, whereas the transition to the R_3R_3' state is effectively prevented due to the unfavorable, (negatively cooperative) energy barrier introduced by the unfavorable value of L_o^B (Figure 3, trace e). Of course, it is theoretically possible to complete the transition to the R_3R_3' conformation provided the ligand concentration can be made sufficiently high. However, ligand solubility can impose a limitation that gives rise to apparent half-site reactivity. The sigmoidal character of the isotherms at low ligand concentrations is primarily determined by the allosteric constant, L_o^A. Shifting the preexisting equilibrium in favor of the T_3T_3' state (i.e., raising L_o^A) raises the energy barrier for anionic ligand binding, and therefore, increased concentrations of anionic ligands are required to shift the conformational equilibrium to the $T_3^oR_3^o$ and R_3R_3' conformations.

Another limiting case of the SMB model that gives rise to an approximate MWC model occurs when L_o^A is very large and L_o^B is very small. Under these conditions, the $T_3^oR_3^o$ conformation is highly destabilized and, thus, does not accumulate during the allosteric transition of the hexamer. Mathematically, this can be expressed as follows: Since $L_o^A = [T_3T_3']/[T_3^oR_3^o]$ and $L_o^B = [T_3^oR_3^o]/[R_3R_3']$, the equilibrium between T_3T_3' and R_3R_3' is defined by $[T_3T_3']/[R_3R_3'] = L_o^A L_o^B$. In the case where L_o^A is very large (e.g., 1×10^{20}) and L_o^B is very small (e.g., 1×10^{-19}), the overall equilibrium between T_3T_3' and R_3R_3' becomes $[T_3T_3']/[R_3R_3'] = L_o^A L_o^B = 10$. Since, in this case, the $T_3^oR_3^o$ conformation is very unfavorable, this species can be treated mathematically as insignificant, and the degree of cooperativity (sigmoidicity) becomes a function of the T_3T_3' to R_3R_3' equilibrium and ligand affinities.

(D) Heterotropic Interactions. Heterotropic ligands can behave as positive, negative, or mixed effectors, depending on how the overall conformational equilibrium is altered. The known heterotropic effectors of phenolic ligand binding, small monovalent anions such as Cl^-, SCN^-, and $PABA^-$, selectively bind to the HisB10 metal ion sites of the R_3, R_3', and R_3^o trimeric units (Brader et al., 1991; Choi et al., 1993; Brzovic et al., 1994; Bloom et al., 1995). Positive heterotropic effectors act by stabilizing either the $T_3^oR_3^o$ or the R_3R_3' states. Spectroscopic investigation and crystal structure analysis of hexamers comprised of R_3, R_3', and R_3^o units show the anion binding sites to be essentially identical (Bloom et al., 1997). Thus, binding of anions acts to stabilize both the $T_3^oR_3^o$ and the R_3R_3' conformations (viz., Figure 1). Since the R_3R_3' conformation has two binding sites, mass action favors this state. Negative heterotropic effectors act by stabilizing either the $T_3^oR_3^o$ or the T_3T_3' conformations. By favoring a state with a reduced number of (phenolic) ligand binding sites, an antagonistic condition will result. Although no anions exhibiting negative heterotropic behavior have been identified, negative heterotropic interactions have been observed between 2,6-DHN and SCN^-. The SMB model allows a ligand to be both a positive and a negative heterotropic effector within the same system. For example, 2,6-DHN is a positive effector of SCN^- binding to the wild-type $T_3^oR_3^o$ conformation, where binding does not exceed half of the sites experimentally. Phenol is a positive effector of SCN^- binding to the R_3R_3' hexamer. However, addition of 2,6-DHN to the wild-type SCN^- adduct of the R_3R_3'-$(phenol)_6$ hexamer results in conversion to the SCN^- adduct of the $T_3^oR_3^o(2,6\text{-DHN})_3$ state. SCN^- is therefore released from half of the sites in a negative heterotropic manner. According to these criteria, and depending on which transi-

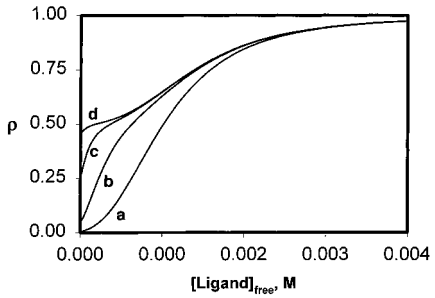

FIGURE 4: Theoretical binding isotherms for the E-B13Q mutant insulin hexamer depicting the influence of heterotropic interactions on curve shape. The following values of the allosteric parameters were used to generate the curves: $L_o^B = 500$, $K_R^o = K_R = 0.0002$ M, and $L_o^A = 100$ (a), 10 (b), 1.0 (c), and 0.1 (d).

tion is considered, 2,6-DHN is both a positive and a negative heterotropic effector of SCN^- binding.

The influence of heterotropic effects on the shapes of the binding isotherms and the distribution of T- and R-state forms in the absence of phenolic ligands is modeled in Figure 4. As a consequence of the heterotropic interactions between the phenolic pockets and the HisB10 anion binding sites, the binding of different anions to the HisB10 sites of T_3R_3 and R_6 significantly alters the apparent values of L_o^A and L_o^B (eq 8 and Figure 1). Using eq 9 and values of $L_o^B = 500$ and $K_R^o = K_R = 2 \times 10^{-4}$ M, Figure 4 shows the theoretical curves for values of $L_o^A = 0.1$, 1.0, 10, and 100. As the value of L_o^A decreases from 100 to 0.1, these simulations show that the fraction of R-state (ρ) initially present (as measured by the ordinate intercept in the absence of ligand) increases from a value near 0 to a value near 0.5, a behavior similar to that observed in Figure 1. Notice that so long as $1/L_o^A >> 1/L_o^A L_o^B$, the distribution of forms in the absence of phenolic ligands is insensitive to the value of L_o^B.

Application of the SMB Model to Other Systems. Although the various allosteric interactions in the insulin hexamer can be described by the SMB model, it is useful to consider whether or not these properties can be applied to other allosteric systems. As observed by Seydoux et al. (1974) and Matthews and Bernhard (1973) more than 20 years ago, there are a large number of oligomeric proteins that adopt a "pairwise asymmetry" that is coupled to an exact symmetry axis, and a significant number of these are observed to possess negative or half-site reactivity. It would appear there are few examples of oligomeric proteins with ligand binding properties that cannot be explained by the SMB model. X-ray analysis of oligomeric proteins such as insulin, hemoglobin, GAPDH, and phosphofructokinase have shown that a pairwise asymmetry is present (Matthews & Bernhard, 1973; Shirakihara & Evans, 1988). Recent publications (Beimann & Koshland, 1994; England & Hervé, 1994, 1992; Hervé, 1989) have put forward possible mechanisms by which negative cooperativity or the half-site reactivity phenomenon must occur, and most cite a sequential (KNF-type) induced-fit process as the mechanism of choice, because ... "negative cooperativity is (thus) a diagnostic test of the KNF model" (Fersht, 1985). One publication has claimed that a definitive test of the sequential versus concerted models has been accomplished for a dimeric binding protein which was crystallized with exactly one ligand per dimer (Beimann & Koshland, 1994). The two active sites exhibited differences in the side chain residues for the ligand-bound state and the water-occupied state. Whether the differences in sites and the half-site binding behavior are induced by ligand binding or are due to a preexisting structural asymmetry cannot be ascertained from this structure. Regardless of the nature of the half-site binding behavior, a dimeric binding protein provides a degenerate system which cannot be used to distinguish between a symmetry/asymmetry-driven process and a sequential, ligand-induced process; when applied to a dimer, both allosteric models involve the same number of conformational states. Most of the examples of negative cooperativity (and half-site reactivity) are described as possessing two classes of sites with different affinities (Seydoux et al., 1974; Koshland et al., 1966; Hervé, 1989; Shirakihara & Evans, 1988; Deville-Bonne & Garel, 1992; Beimann & Koshland, 1994). Solubility limits and solvent effects are common limitations to determining the affinities of weak binding sites. It is difficult to obtain accurate and complete isotherms in negative cooperative systems. Because complete binding to both phases of the ligand binding isotherms can be attained, the insulin hexamer is the first well-characterized system that can differentiate between the KNF and SMB models. The evidence of a preexisting equilibrium consisting of T- and R-state species in the absence of anionic and phenolic ligands (Choi et al., 1996) effectively rules out a KNF model. This work and the preceding paper (Bloom et al., 1997) demonstrate that the SMB model provides an attractive quantitative model which takes into consideration the structural properties of the insulin hexamer. In the past 5 years, the insulin hexamer has been extensively studied by both crystallographic and biophysical means. These studies have revealed that the system possesses a wealth of information regarding the mechanisms of cooperativity. To our knowledge, it is the first example of a ligand binding system that exhibits both negative and positive cooperative behavior and has been quantitatively and qualitatively assigned an allosteric mechanism that is based on asymmetry/symmetry constraints.

APPENDIX

The Mathematical Model: Derivation of Analytical Expressions for the SMB Model Tailored to the Insulin Hexamer. To achieve a quantitative description of the interactions of phenolic compounds (P) with the insulin hexamer, we define the possible ligation states as follows: Prior to ligand binding, the hexamer is capable of existing in three states, T_3T_3', $T_3^oR_3^o$, and R_3R_3', which herein are designated T_0, Z_0, and R_0, respectively [as per the nomenclature of Monod et al. (1965)]. Since no binding of ligand can occur to the T_3T_3' conformation, T_0 is the only T-form necessary for this analysis. The notation Z_0, Z_1, Z_2, and Z_3 and Q_0, Q_1, Q_2, Q_3, ..., Q_6 is used to denote hexameric species with 0, 1, 2, 3 ..., 6 molecules of ligand bound, where Z designates bound subunits in the R^o conformational state and Q designates bound subunits in the R or R′ conformational states. The equilibria can be written as shown in Scheme 1.

Since each type of site within a given conformation state has identical and independent microscopic affinities and there are multiple sites in each state, statistical coefficients for

Scheme 1

$$Z_0 \rightleftharpoons Q_0$$

$$Z_0 + P \rightleftharpoons Z_1 \qquad Q_0 + P \rightleftharpoons Q_1$$

$$Z_1 + P \rightleftharpoons Z_2 \qquad Q_1 + P \rightleftharpoons Q_2$$

$$Z_2 + P \rightleftharpoons Z_3 \qquad Q_2 + P \rightleftharpoons Q_3$$

$$Q_3 + P \rightleftharpoons Q_4$$

$$Q_4 + P \rightleftharpoons Q_5$$

$$Q_5 + P \rightleftharpoons Q_6$$

ligand binding and dissociation in the equilibria shown in Scheme 2 are required for each of the complexes. Two

Scheme 2

$$[Z_1] = [Z_0](3/1)([P]/K_R^{o}) \qquad [Q_1] = [Q_0](6/1)([P]/K_R)$$

$$[Z_2] = [Z_1](2/2)([P]/K_R^{o}) \qquad [Q_2] = [Q_1](5/2)([P]/K_R)$$

$$[Z_3] = [Z_2](1/3)([P]/K_R^{o}) \qquad \vdots$$

$$[Q_6] = [Q_5](1/6)([P]/K_R)$$

additional functions can be defined, corresponding to (a) the fraction of monomers in the R-state (ρ)

$$\rho = \frac{3[Z_0 + Z_1 + Z_2 + Z_3] + 6[Q_0 + Q_1 + Q_2 + ... + Q_6]}{6[Z_0 + Z_1 + Z_2 + Z_3] + 6[Q_0 + Q_1 + Q_2 + ... + Q_6] + 6T_0} \quad (9)$$

and (b) the fraction of sites actually bound by ligand

$$Y_F = \frac{Z_1 + 2Z_2 + 3Z_3 + Q_1 + 2Q_2 + ... + 6Q_6}{6[Z_0 + Z_1 + Z_2 + Z_3] + 6[Q_0 + Q_1 + Q_2 + ... + Q_6] + 6T_0} \quad (10)$$

By inserting the equilibrium equations and setting

$$([P]/K_R^{o}) = \beta \qquad ([P]/K_R) = \alpha \quad (11)$$

the equation for the fraction of R-state becomes

$$\rho = \frac{0.5L_o^{B}(1+\beta)^3 + (1+\alpha)^6}{L_o^{B}(1+\beta)^3 + (1+\alpha)^6 + L_o^{A}L_o^{B}} \quad (7)$$

and the fraction of saturation function becomes

$$Y_F = \frac{0.5L_o^{B}\beta(1+\beta)^2 + \alpha(1+\alpha)^5}{L_o^{B}(1+\beta)^3 + (1+\alpha)^6 + L_o^{A}L_o^{B}} \quad (12)$$

Equation 7 provides a convenient analytical expression both for modeling the SMB model applied to the insulin hexamer system and for fitting experimental data such as those reported in Figure 1.

REFERENCES

Baker, E. N., Blundell, T. L., Cutfield, J. F., Cutfield, S. M., Dodson, E. J., Dodson, G. G., Hodgkin, D. C., Hubbard, R. E., Isaacs, N. W., Reynolds, C. D., Sakabe, K., Sakabe, N., & Vijayan, N. M. (1988) *Philos. Trans. R. Soc. London, B 319*, 369−456.

Beimann, H.-P. & Koshland, D. E. (1994) *Biochemistry 33*, 629−634.

Bloom, C. R., Choi, W. E., Brzovic, P. S., Ha, J. J., Huang, S.-T., Kaarsholm, N. C., & Dunn, M. F. (1995) *J. Mol. Biol. 245*, 324−330.

Bloom, C. R., Heymann, R., Kaarsholm, N. C., & Dunn, M. F. (1997) *Biochemistry 36*, 12746−12758.

Brader, M. L., Kaarsholm, N. C., Lee, R. W.-K., & Dunn, M. F. (1991) *Biochemistry 30*, 6636−6645.

Brzovic, P. S., Choi, W. E., Borchardt, D., Kaarsholm, N. C., & Dunn, M. F. (1994) *Biochemistry 33*, 13057−13069.

Choi, W. E., Brader, M. L., Aguilar, V., Kaarsholm, N. C., & Dunn, M. F. (1993) *Biochemistry 32*, 11638−11645.

Choi, W. E., Borchardt, D., Kaarsholm, N. C., Brzovic, P. S., & Dunn, M. F. (1996) *Proteins: Struct., Funct., Genet. 26*, 377−390.

Ciszak, E., & Smith, G. D. (1994) *Biochemistry 33*, 1512−1517.

Derewenda, U., Derewenda, Z., Dodson, E. J., Dodson, G. G., Reynolds, C. D., Smith, G. D., Sparks, C., & Swensen, D. (1989) *Nature 338*, 594−596.

Deville-Bonne, D., & Garel, J.-R. (1992) *Biochemistry 31*, 1695−1700.

Eisenstein, E. Markby, D. W., & Schachman, H. K. (1990) *Biochemistry 29*, 3724−3731.

England, P., & Hervé, G. (1992) *Biochemistry 31*, 9725−9732.

England, P., & Hervé, G. (1994) *Biochemistry 33*, 3913−3918.

Fersht, A. (1985) *Enzyme Structure and Mechanism*, Freeman and Co., New York.

Hervé, G. (1989) in *Allosteric Enzymes* (Hervé G., Ed.) CRC Press, Boca Raton, FL.

Kaarsholm, N. C., Ko, H.-C., & Dunn, M. F. (1989) *Biochemistry 28*, 4427−4435.

Koshland, D. E., Nemethy, G., & Filmer, D. (1966) *Biochemistry 5*, 365−385.

Kuo, L. C., Zambidis, I., & Caron, C. (1989) *Science 245*, 522−524.

Matthews, B., & Bernhard, S. A. (1973) *Annu Rev. Biophys. Bioeng. 2*, 257−317.

Monod, J., Wyman, J., & Changeux, J.-P. (1965) *J. Mol. Biol. 12*, 88−118.

Roy, M., Brader, M. L., Lee, R. W.-K., Kaarsholm, N. C., Hansen, J., & Dunn, M. F. (1989) *J. Biol. Chem. 264*, 19081−19085.

Seydoux, F., Malhotra, O. P., & Bernhard, S. A. (1974) *CRC Crit. Rev. Biochem. 2*, 227−257.

Shirakihara, Y., & Evans, P. R. (1988) *J. Mol. Biol. 204*, 973−994.

Smith, G. D., & Dodson, G. G. (1992a) *Biopolymers 32*, 1749−1756.

Smith, G. D., & Dodson, G. G. (1992b) *Proteins: Struct., Funct., Genet. 14*, 401−408.

Smith, G. D., Swenson, D. C., Dodson, E. J., Dodson, G. G., & Reynolds, C. D. (1984) *Proc. Natl. Acad. Sci. U.S.A. 81*, 7093−7097.

Stebbens, J. W., & Kantrowitz, E. R. (1992) *Biochemistry 31*, 2328−2332.

Whittingham, J. L., Chaudhuri, S., Dodson, E. J., Moody, P. C. E., & Dodson, G. G. (1995) *Biochemistry 34*, 15553−15563.

BI970762F